Article

Exploring the Role of NH_4Cl Supplementation on Triacylglycerol Production by *Chlamydomonas reinhardtii* under Mixotrophic Cultivation using a Proteomics Approach

Wattanapong Sittisaree [1], Kittisak Yokthongwattana [1], Chanat Aonbangkhen [2], Yodying Yingchutrakul [3*] and Sucheewin Krobthong [2,4*]

[1] Department of Biochemistry, Faculty of Science, Mahidol University, Bangkok, 10400, Thailand; wattanapong.sit@gmail.com (W.S) and kittisak.yok@mahidol.edu (K.Y.)
[2] Center of Excellence in Natural Products Chemistry (CENP), Department of Chemistry, Faculty of Science, Chulalongkorn University, Bangkok 10330, Thailand, chanat.a@chula.ac.th
[3] National Omics Center, NSTDA, Pathum Thani, 12120, Thailand, yodying.yin@nstda.or.th
[4] Center for Neuroscience, Faculty of Science, Mahidol University, Bangkok, 10400, Thailand; sucheewin82@gmail.com
* Correspondence: sucheewin82@gmail.com (S.K.) and yodying.yin@nstda.or.th (Y.Y)

Simple Summary: Because NH4Cl is one of the nitrogen sources for microalgal cultivation, its use as a supplement for triacylglycerol production is anticipated to have wide-ranging benefits, both anticipated and unanticipated. In our study revealed NH_4Cl supplementation under mixotrophic conditions has the potential to increase biomass and lipid production in microalgal cultures. To sum it up, we conclude that this article can provide increased biochemical knowledge so that microalga development can be more efficiently used as a sustainable energy source. We find this to be very exciting and we hope to share this information with your readership.

Abstract: NH_4Cl is one of the nitrogen sources for microalgal cultivation. However, excessive amounts of NH_4Cl affects microalgal physiology and biomass contents. In this study, the effects of ammonium on microalgal growth and TAG content in the green microalga (*Chlamydomonas reinhardtii*) was investigated. Microalgal growth and TAG content under photoautotrophic conditions were found to be unchanged with 17 mM of ammonium, while this compound interfered with microalgal growth and induced TAG content under mixotrophic conditions with acetate supplementation. This suggested that ammonium could induce TAG production when acetate occurred in microalgal cultivation. Further, the effects of two different concentrations of NH_4Cl (17 mM and 60 mM) on the cells under mixotrophic conditions were investigated. The results showed that both concentrations reduced microalgal growth, but induced total lipid and TAG content, especially after a 4-day cultivation. The oxygen evolution and Fv/Fm ratio showed that both concentrations completely inhibited the oxygen evolution on Day 4. The 60 mM NH_4Cl reduced the Fv/Fm ratio from 0.7 to 0.48 indicating that ammonium supplementation directly affects the microalgae photosynthesis performance. A total of 1782 proteins were successfully identified using proteomics analysis. Among them, there were nine overexpressed proteins and four proteins were underexpressed. Using the protein–ligand interaction analysis, nitrogen metabolism is involved under NH_4Cl conditions. This information can provide biochemical knowledge for microalgae development for sustainable energy usage.

Keywords: microalgae; biomass; photosynthesis; mixotrophic; renewable energy; LC-MS/MS

 doi:10.20944/preprints202211.0284.v1

1. Introduction

The global energy crisis is worsening. To address this serious problem, sustainable, alternative energy sources should be used instead of nonrenewable energy. Microalgae are a source of mass-production of energy-rich oil or biofuels [1]. Various microalgae can accumulate a high number of storage fuels, starch, and lipid, including methane, hydrogen, ethanol, and triglycerides (TAG) for energy usage higher than general plants [2,3]. Biodiesel from microalgae is an accepted high-quality biofuel because it does not contain sulfur and reduces carbon monoxide and hydrocarbon emissions. Several microalgae have been reported to apply in biodiesel production, such as *Chlorella, Dunaliella, and Tetraselmis* because they can accumulate oil content ranging from 20% to 50% and reach high productivity [1,4,5].

Microalgae has many interesting aspects for biofuel production; for example, fast-growing, high biomass and high lipid, and TAG production. Among these aspects, TAG induction in microalgae is the most appropriate way to improve microalgal biofuel production [6] Extreme environmental and operational factors can affect microalgal biomass productivity, biomass compositions, as well as lipid and TAG content, such as nutrient starvation and abiotic stresses [7,8]

Nitrogen is an important nutrient for microalgal biomass production because of its significant influence on microalgal growth, which is dependent upon the amount, availability, and nitrogen source type [9]. Ammonium is toxic to cells at elevated concentrations and can cause growth inhibition or even cell death despite it being the preferred microalga nitrogen source [10,11]. However, ammonium toxicity in microalgae can be alleviated by the addition of carbon sources, such as glucose and acetate [12]. Under carbon supplementation, the ammonium assimilation is increased leading to reduced ammonium toxicity. Moreover, mixotrophic cultivation with ammonium could greatly enhance microalgal growth, biomass, total lipid, and particularly TAG content [13,14].

TAG is a class of nonpolar lipids that are regarded as a sustainable feedstock for the chemical, food, and biofuel industries. In microalgae, the TAG biosynthesis pathway requires many enzymatic reactions involving numerous cellular compartments. Generally, proteins regulate various biochemical mechanisms of cellular processes, such as molecular extracellular and intracellular cell response, cell movement, cell trafficking, cell catabolism and anabolism, cell maintenance, and lipid biosynthesis. Proteomics is a technique used to identify and characterize all proteins expressed simultaneously under different conditions. The most commonly used methods for quantitative proteomes are label-free-based proteomics coupled with LC-MS/MS because of their performance and reliable method for large-scale protein identification and quantification. In this study, NH_4Cl's effect on the TAG content in photoautotrophic and mixotrophic in *C. reinhardtii* was investigated. The NH_4Cl's effect on triglyceride content under mixotrophic condition was also investigated, analyzed the underlying adaptation mechanisms, and proposed a model by a proteomic approach in a model green microalga. The information can be useful for microalgae development for sustainable energy usage.

2. Materials and Methods

2.1. Microalgal growth conditions and experimental designs

The microalgae used in this study were *C. reinhardtii* CC125. *C. reinhardtii* was grown in tris-minimal medium for photoautotrophic and tris-acetate phosphate (TAP) medium for mixotrophic cultivation. Temperature was controlled at 24 2.6 C. Light was illuminated and controlled to constant intensities at 50 µmol photons m^{-2} s^{-1} throughout the experiment using tungsten halogen light source (1500 W) (Matsushita, Japan). To test the ammonium chloride, this compound's concentration was varied (0, 17, and 60 mM).

2.2. Growth characteristics and biomass determination

Growth characteristics were measured using cell counting by hemocytometer every 24 h until reaching the stationary phase. Biomass was measured in terms of dry weight.

Preprints (www.preprints.org) | NOT PEER-REVIEWED | Posted: 15 November 2022 doi:10.20944/preprints202211.0284.v1

A 10 mL microalgal culture was filtered through 0.22-μM nylon membrane filter. To estimate the microalgal biomass on the filters, the following equations were calculated:

Biomass concentration (g/cell) = (Final weight filter − initial weight filter)/cell number

Biomass dry weight (g/ml) = (Final weight filter − initial weight filter)/microalgal medium volume

Biomass productivity (mg/l/d) = (Final weight filter − initial weight filter)/(microalgal medium volume)(day of microalgal growth)

2.3. Photosynthesis activity measurement

Photosynthesis activity was measured based on PSII quantum efficiency, microalgal cell aliquots 3 mL were collected daily from the algal cultures, and incubated in the dark for 10 min pre-experiment. The Fv/Fm ratio using a fluorometer (Z985 Cuvette AquaPen, Qubit Systems, Ontario, Canada) was used to measure PSII quantum efficiencies. A Clark-type electrode model OX1LP dissolved O_2 package (Qubit Systems, Canada) was used to determine the rate of O_2 evolution. O_2 evolution rates were monitored for 1 min each at individual light irradiance from 0 to 1000 μmol photons m^{-2} s^{-1}. Photosynthesis activity was measured based on chlorophyl a and chlorophyl b abundance. The chlorophyll contents in the microalgal cells were extracted using 80% acetone for 10 min. Cell debris was removed by centrifugation at 14,000 × g for 10 min. Spectrophotometry was used to measure the pigment concentration at 663.2, 646.8, and 470 nm. The pigment concentration was calculated using referenced equation [15].

2.4. Total lipid and TAG measurements

The microalgal cells (1.75×10^8 cells) were extracted using chloroform and methanol (1:2 v/v) according to modified by Bligh and Dyer (Ref2) for lipid content determination. The supernatant from the extraction was transferred to a 10-mL test tube and evaporated by airflow for 72 h at room temperature. The amount of lipid was measured gravimetrically and calculated using the following equations:

Lipid content (g/cell) = (Final weight test tube − initial test tube)/cell number

Lipid productivity (mg/l/d) = (Final weight test tube − initial test tube)/(microalgal medium volume)(day of microalgal growth)

The TAG content was analyzed by thin-layer chromatography (TLC). The extracted cells were dissolved in chloroform: methanol (1:2 v/v) into a final volume of 200 μL. Soybean oil (1 μg/μL) concentration was used as a reference standard for TAG. A TLC plate (Silica gel 60 F254, Merck) was used to spot the testing sample and soybean oil standard. The mobile phase composed of hexane: diethyl ether: acetic acid (70:30:1 v/v/v) was performed. Iodine vapor standing for 30 min was done for lipid band visualization. The amount of TAG was measured and calculated using the following equations:

TAG content (g/cell) = Weight of TAG/cell number

TAG productivity (mg/l/d) = Weight of TAG/(microalgal medium volume)(day of microalgal growth)

2.5. Sample preparation for proteomics analysis

The alga cells were prepared for proteomics using a previously published protocol with minor modifications [16,17]. Briefly, the cells were lysed on ice using a probe tip sonication at a frequency of 20 kHz and 80% amplitude for 2 s on and 3 s off for a total of 15 s in 200 μl lysis buffer (0.2% TritonX-100, 10 mM DTT, 5 mM sodium chloride, 10 mM HEPES-KOH, pH 8.0) with protease inhibitor cocktail. The protein solution was collected by centrifugation at 15,000 g for 30 min and subsequent to ice-cold 15% TCA/acetone precipitation (1:5 v/v) for 16 h. After precipitation, the pallet protein was reconstituted in 0.3%

 doi:10.20944/preprints202211.0284.v1

RapidGest SF (Waters, UK) and 5 mM NaCl in 5 mM ammonium bicarbonate. A total of 45 μg protein was subjected to gel-free based digestion. Sulfhydryl bonds were reduced using 5 mM DTT in 5 mM ammonium bicarbonate at 80°C for 1 h and sulfhydryl group alkylation using 15 mM IAA in 5 mM ammonium bicarbonate at room temperature for 40 min in the dark. The solution was cleaned up using a desalting column (Zeba™ Spin Desalting Columns, 7K MWCO, 0.5 mL, ThermoFisher). The flow-through solution was enzymatically digested by trypsin (Promega, Germany) at a ratio of 1:40 (enzyme: protein) and incubated at 37°C for 6 h. The tryptic peptides were dried and stored at −20°C until analysis.

2.6. LC-MS/MS configurations

The SciEx high resolution 6600+ TripleTOF™ (AB-Sciex, Concord, Canada) coupled to a nanoLC-system: UltiMate 3000 LC System (Thermo Fisher Scientific, USA) was used to analyze the proteomics analysis. The dried tryptic peptides were reconstituted with 0.1% formic acid. A total of 1.2 μg protonated peptides was subjected to the nanoLC-system. LC conditions are as follows: mobile phase A composed of 0.1% formic acid in water and mobile phase B composed of 90% acetonitrile with 0.1% formic acid. The samples were loaded directly onto the Analytical column C_{18} (Reverse phase chromatography) separation (2 mm, 75 μm × 15 cm) and separated according to 145 min at a constant flow rate of 300 nl/min. The mass spectrum was acquired in a data-dependent acquisition mode. MS full scans over a mass range of 400–1600 *m*/*z* of which the top 30 most abundant peptide ions, with a charged state in the range of 2–5 *m*/*z*, were selected for fragmentation. The dynamic exclusion duration was set at 18 s. The Paragon™ Algorithm by ProteinPilot™ Software [18] was used to extract and annotate with protein sequences the raw MS-spectra resulting (.wiff) file. The *Chlamydomonas* retrieved from the UniprotKB database used in Paragon™ was assembled in FASTA format downloaded on February 17, 2022. The normalization of protein abundance data was performed using NormalyzerDE [19], in which quantile-normalization is applied to relative expression data analysis, after adding "1" to all expression values to avoid errors upon log-transformation. Only proteins identified at FDR ≤ 1% with ≥ 10 peptides/protein were considered for the protein lists.

2.7. Statistical analysis

All testing factors were carried out with at least three independent replicates (n = 3) and data were reported as mean ± standard deviation. The GraphPad Prism version 8.01 (GraphPad Software, San Diego, CA, United States) was used to perform the statistical analyses of all data. The significance is indicated with an asterisk ($p \leq 0.05$), double asterisk ($p \leq 0.01$), or triple asterisk ($p \leq 0.001$).

For the pairwise comparisons in proteomics analysis, a one-way analysis of variance (one-way ANOVA) at protein-level analysis with two multiple testing correction methods, including the Bonferroni correction and the Benjamini and Hochberg FDR-correction, was performed using the ProteinPilot™ Software.

3. Results

3.1. NH_4Cl supplementation effect on C. reinhardtii growth and TAG content under photoautotrophic and mixotrophic conditions

The NH_4Cl effect on *C. reinhardtii* growth, biomass, and TAG content was investigated under photoautotrophic and mixotrophic conditions. Under the photoautotrophic condition, microalgal cell growth showed that 17 mM NH4Cl did not reduce microalgal growth when compared to the control conditions (Fig. 1A).

Preprints (www.preprints.org) | NOT PEER-REVIEWED | Posted: 15 November 2022 doi:10.20944/preprints202211.0284.v1

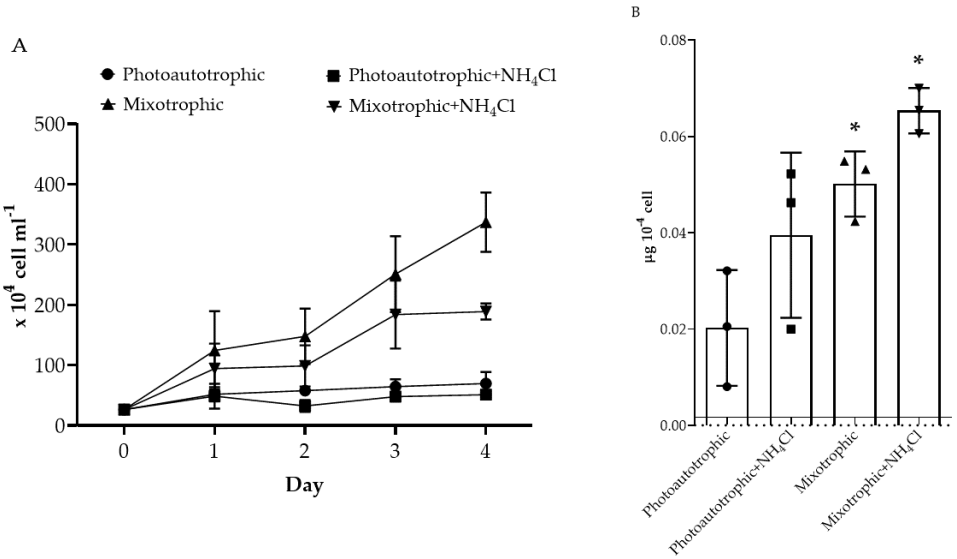

Figure 1. Effect of NH_4Cl on *C. reinhardtii* growth and biomass production under photoautotrophic and mixotrophic conditions. (A) Microalgal cell number. (B) TAG production.

However, 17 mM NH_4Cl decreased microalgal growth under the mixotrophic conditions. Biomass (Fig. 1B) evaluation of cellular TAG content showed that NH_4Cl did not increase cellular TAG content under photoautotrophic conditions. However, NH_4Cl significantly increased microalgal cellular TAG content under mixotrophic conditions (Fig. 1C and 1D).

3.2. Effect of NH_4Cl supplement and growth characteristic and TAG content on C. reinhardtii under mixotrophic conditions

The NH_4Cl concentration and microalgal growth phase were investigated to further study the NH_4Cl effect on TAG content in the cells under mixotrophic condition. Microalga was cultivated in standard TAP media under mixotrophic conditions. For the NH_4Cl supplement, the microalgal culture was added to 17 mM and 60 mM NH_4Cl. The growth, biomass, total lipid, and TAG content were measured after 48 and 96 h. Microalgal growth showed that treatment with 17 mM and 60 mM NH_4Cl decreased cell density since the exponential growth phase. However, the effects between 17 mM and 60 mM ammonium treatment on microalgal growth were not different (Fig. 2A).

Preprints (www.preprints.org) | NOT PEER-REVIEWED | Posted: 15 November 2022 doi:10.20944/preprints202211.0284.v1

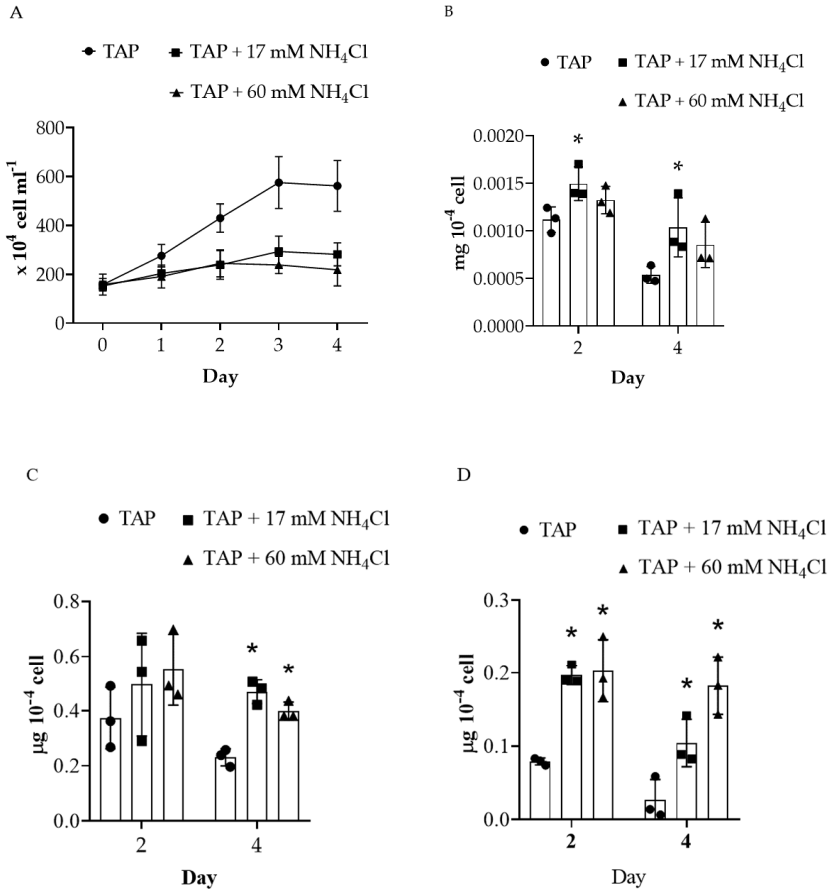

Figure 2. Comparison of microalgal biomass production under NH_4Cl at the exponential and stationary growth phases. A) Cell concentration. B) Total cell dry weight. C) Total lipid production. D) TAG production. (C) *C. reinhardtii* productivity under batch cultivation under different growth conditions.

Characterization of biomass dry weight showed that only 17 mM NH_4Cl treatment significantly increased the microalgal biomass at the exponential growth phase. In addition, both 17- and 60-mM ammonium supplement increased microalgal biomass at the stationary growth phase (Fig. 2B).

The total cellular lipid and cellular TAG contents were measured. The results showed that NH_4Cl at both concentrations did not affect the cellular TAG contents at the exponential growth phase, but it significantly increased the total cellular lipid content at the stationary growth phase (Fig. 2C). The cellular TAG content was significantly increased after both 17 and 60 mM NH_4Cl at the exponential and stationary growth phases. However, the NH_4Cl supplementation effect at both concentrations on cellular triglyceride content was not significantly different.

3.3. Ammonium effect on C. reinhardtii photosynthesis performance under mixotrophic conditions

Photosynthesis efficiency was investigated by various parameters, including photosynthesis rate (O_2 evolution), photorespiration rate (O_2 consumption), the photosystem II maximum quantum efficiency (Fv/Fm ratio), and chlorophyl content determination.

The photosynthesis capacity was characterized by O_2 evolution. O_2 evolution is the process of oxygen production involved in the photochemical reaction in the photosynthesis machinery. The O_2 evolution rate was measured at the exponential growth and stationary growth phases. The photosynthesis capacity was normalized by microalgal cell number and chlorophyl content (Fig. 3A).

Preprints (www.preprints.org) | NOT PEER-REVIEWED | Posted: 15 November 2022 doi:10.20944/preprints202211.0284.v1

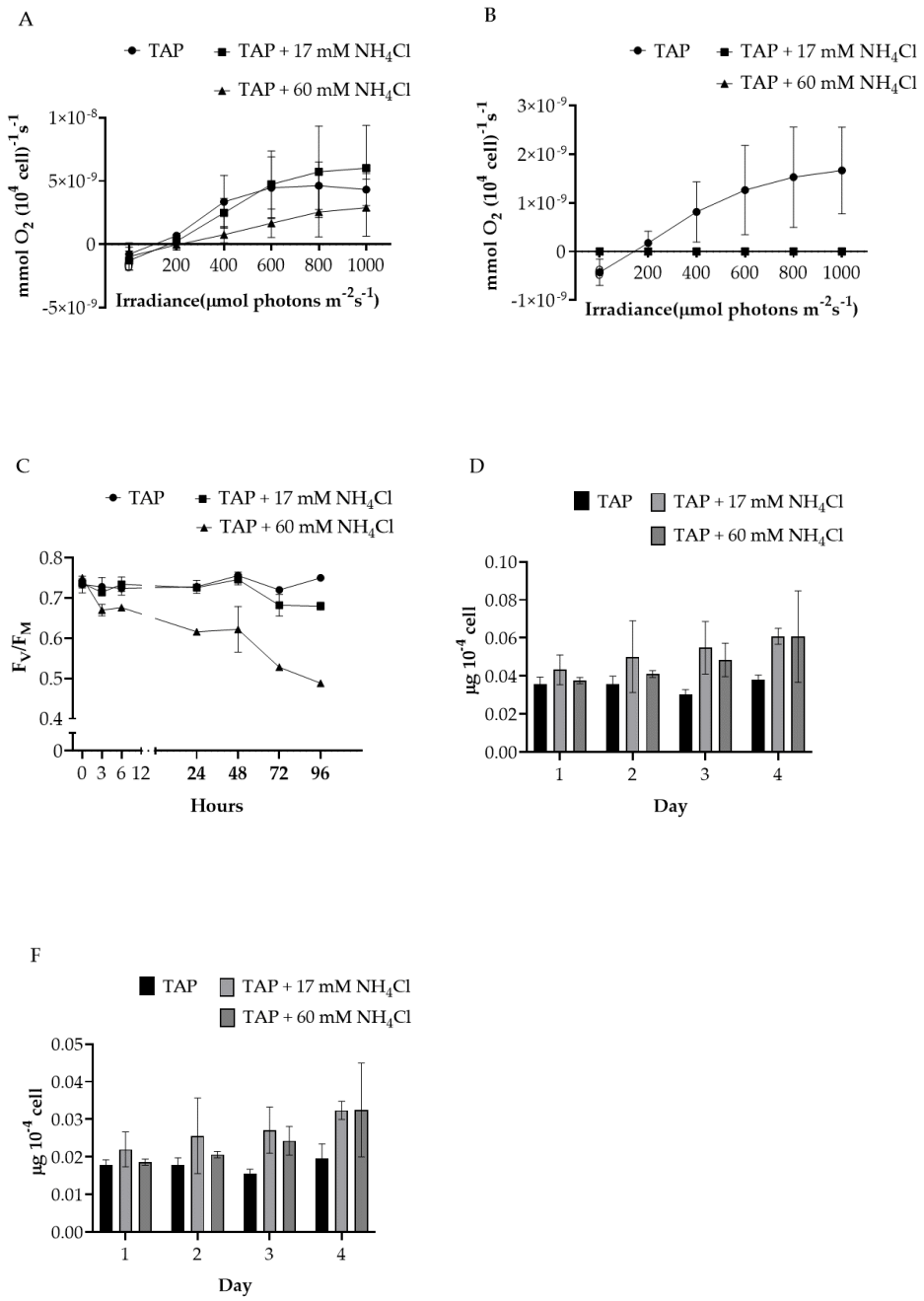

Figure 3. NH_4Cl's effect on photosynthesis parameters. A) O_2 evolution at the exponential growth phase and (B) at the stationary growth phase. C) Fv/Fm ratio. D) Chlorophyll a content. F) Chlorophyll b content.

At the exponential growth phase, the photosynthesis rates linearly increased under standard TAP media with increasing light intensity from 0 to 400 µmol photon m^{-2} s^{-1}. The photosynthesis rate reached the saturated level at around 600 µmol photon m^{-2} s^{-1}. The maximum photosynthesis rate was approximately 5×10^{-9} mmol O_2 $(10^4$ cell$)^{-1}$. For 17 mM ammonium treatment, the photosynthesis rate showed a similar trend to that of the standard TAP media cultivation. However, the cells' photosynthesis rate under 60 mM NH_4Cl treatment tended to decrease. At the stationary growth phase, the microalgal cells' photosynthesis rates linearly increased under standard TAP media with increasing light intensity from 0 to 400 µmol photon m^{-2} s^{-1}. Then, the photosynthesis rates reached the saturated level at around 600 µmol photons m^{-2} s^{-1} (Fig. 3B). However, the maximum

Preprints (www.preprints.org) | NOT PEER-REVIEWED | Posted: 15 November 2022 doi:10.20944/preprints202211.0284.v1

photosynthesis rate was decreased when compared to the photosynthesis rate at the exponential growth phase. The maximum is approximately 1.5×10^{-9} mmol O_2 $(10^4$ cell$)^{-1}$.

The Fv/Fm ratio from the *C. reinhardtii* under 17 mM NH_4Cl showed that this ratio was not changed from the start up to 72 h (Fig. 3C). The Fv/Fm ratio was significantly decreased after 96 h of cultivation. For 60 mM NH_4Cl, the ratio was significantly decreased after 3 h and was completely inhibited at 72 h.

The chlorophyl content was determined. Compared to the standard TAP media cultivation, the 17- and 60-mM NH_4Cl supplementation did not significantly change the chlorophyll a and b content (Fig. 3D and 3F).

3.4. Proteomic analysis of ammonium on triglyceride trigger in Chlamydomonas reinhardtii under mixotrophic conditions

A total of 1782 proteins were identified using LC-MS/MS-based proteomics analysis. According to the Venn diagram (Fig. 5A), nuclear/nucleolar GTPase 2 (A0A2K3DKG5_CHLRE) and nuclear/nucleolar GTPase 2 (Fragment) (A8ITK3_CHLRE) were unique to the 17 mM NH_4Cl condition. Proteomics interpretation showed that 1774 proteins (six proteins were filtered out due to missing expression values) were affected by the NH_4Cl, as shown in the Volcano plot in Fig. 5B. The plot was upregulated (40.81%; for 724/1774 proteins) and downregulated (59.19%; for 1050/1774 proteins).

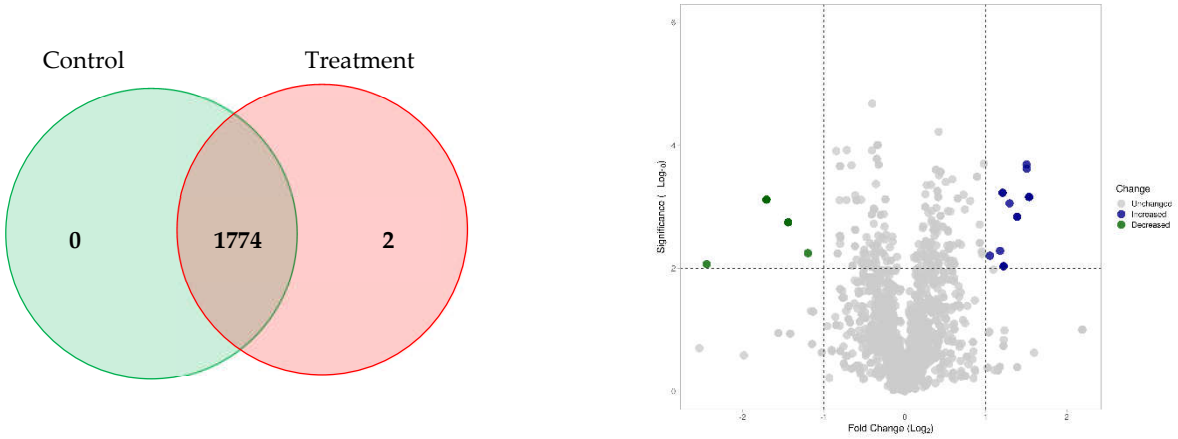

(A) (B)

Figure 4. Proteomics analysis illustrates using Venn-diagram and Volcano plots. (A) Venn diagram shows the protein number identified in each group. (B) The plot shows a negative natural log of the *p*-values plotted against the base2 log values of the change in each protein between the NH_4Cl and control groups. Statistically significant results (p <0.01; −log [p >2]) are plotted above the dashed line. Proteins significantly upregulated and downregulated upon treatment with 17-mM NH_4Cl are shown as blue and green dots, respectively.

The significant protein lists are shown in Table 1. According to Table 1 and Fig. 4B, a stringent comparison between the NH_4Cl and control groups was used; nine proteins were overregulated, and four proteins were downregulated. These proteins' biological functions varied from transportation protein, metabolic process, cellular development, and redox homeostasis. Among these proteins, there were seven proteins that were fully annotated with functionality (uncharacterized proteins were excluded) as shown in Table 1.

Preprints (www.preprints.org) | NOT PEER-REVIEWED | Posted: 15 November 2022 doi:10.20944/preprints202211.0284.v1

Table 1. Quantitative proteome data of proteins with differential abundance (log 2 ratio <1 or >1 relative to the control condition).

Protein name	Accession	adj *p*-value	log_2FC
Putative acetate uptake transporter GFY5	A0A2K3CP19_CHLRE	6.9E-04	1.533
TNase-like domain-containing proteins	A0A2K3E7W0_CHLRE	2.4E-04	1.502
-	A8HN65_CHLRE	2.0E-04	1.502
-	A8I6S0_CHLRE	1.5E-03	1.386
Uncharacterized protein	A8I6R6_CHLRE	8.8E-04	1.293
Acyl-coenzyme A oxidase	A0A2K3DRX6_CHLRE	9.3E-03	1.219
Fe2OG dioxygenase domain-containing proteins	A0A2K3E0R9_CHLRE	5.9E-04	1.207
Uncharacterized protein	A8J635_CHLRE	5.2E-03	1.176
Uncharacterized protein	A8HPM8_CHLRE	6.2E-03	1.051
Uncharacterized protein	A8IVH0_CHLRE	5.7E-03	−1.193
Low-temperature-induced cysteine proteinase-like	A0A2K3DFE4_CHLRE	1.8E-03	−1.437
Pherophorin-C2 protein	Q3HTK5_CHLRE	7.6E-04	−1.705
Peptidylprolyl isomerase	A8J740_CHLRE	8.6E-03	−2.442

Generally, proteins do not act independently. They interact as either transient or stable complexes with their partner proteins. The STITCH protein–ligand prediction tool was used to clarify the NH_4Cl biochemical mechanism in the microalgae (Figure 5). A total of seven fully annotated proteins with two unique proteins (Fig. 4A) with ammonium ions were imported and searched using the *C. reinhardtii* database.

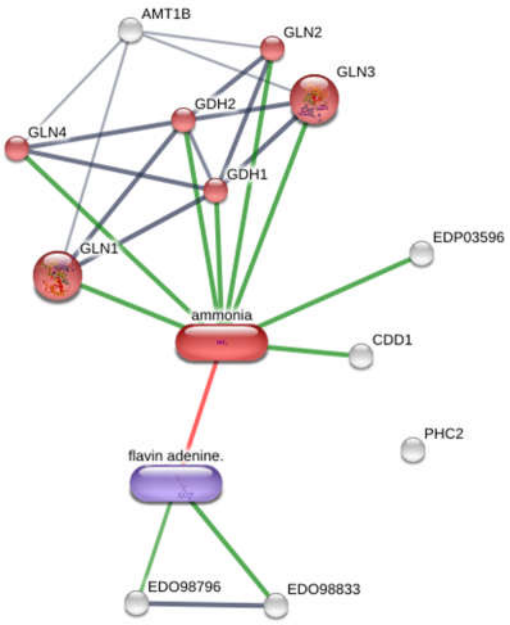

Figure 5. Protein–ligand interaction analysis of significantly expressed proteins in NH_4Cl conditions. The network nodes represent proteins, while the edges represent the predicted functional associations (seven edges) with the interaction score (the threshold of the confidence score was set to 0.4).

The ligand–protein interaction networks are shown in Fig. 5. Functional enrichment analysis revealed that the highest KEGG pathway affected by ammonium ions was nitrogen metabolism (ID: 00910) with FDR = $2.19e^{-13}$. To complete the network, nine proteins

 doi:10.20944/preprints202211.0284.v1

(ED098796, GDH1, CDD1, GLN1, GDH2, GLN4, GLN3, EDP03596, and GLN2) and one ligand (flavin adenine dinucleotide) were recruited in this analysis. Among the six proteins (red node) classified in the nitrogen metabolism, as illustrated in Fig. 6, ammonium ion revealed direct interactions with EDP03596, CDD1, GLNs, and GDH proteins. These interactions suggest that ammonium supplementation can affect cell growth, photosynthesis efficiency, and TAG accumulation by the nitrogen metabolism route.

4. Discussion

NH_4Cl understanding in TAG induction in microalga cells can be applied to improve the microalgal lipid production process and environment bioremediation [20]. The ammonium biochemical mechanisms on microalgal growth and triglyceride production were initially investigated under photoautotrophic and mixotrophic conditions. Photoautotrophic or autotrophic refers to the generation of organic matter and cellular energy by fixing on inorganic carbon. CO_2 in the atmosphere is the primary source of inorganic carbon. In mixotrophic conditions, microalgae are allowed to fix CO_2 and supplement organic carbon sources [3]. NH_4Cl did not alter microalgal growth and TAG production under photoautotrophic conditions. However, it significantly reduced microalgal growth and increased TAG production under mixotrophic conditions. In our study, the mixotrophic condition was supplied by acetic acid (organic carbon source). This might suggest that NH_4Cl triggers TAG with organic carbon supplementation. These results also suggest that acetic acid is one of the crucial factors for TAG production. Corresponding to the other studies in various microalgae species, acetic acid can induce TAG accumulation under normal and nitrogen starvation [21]. Moreover, Goodson and their colleague showed that mixotrophic cultivation by acetate supplementation can increase biomass and lipid accumulation within microalga under nitrogen starvation conditions [22].

To further investigate the effect of NH_4Cl on TAG production under the mixotrophic conditions, this experimental design used 17 mM and 60 mM NH_4Cl. There was no difference in total lipid and TAG production in NH_4Cl supplement conditions. These results confirmed that NH_4Cl can enhance biomass, total lipid, and TAG production in *C. reinhardtii* under acetate ion supplementation. Moreover, the combined effects of acetate ion and ammonium ions have also been reported in *N. oculata*, another microalgae species [23]. This study revealed that the lipid content was enhanced when ammonium ion was used as a nitrogen source, especially in the presence of acetate ions.

To examine NH_4Cl's role in TAG induction under acetate supplementation, the various photosynthesis efficiency parameters were investigated. The photosynthesis rate of microalga at the stationary growth phase under NH_4Cl conditions was completely inhibited. Interestingly, the photosynthesis rate of microalgal cells under ammonium supplement in both NH_4Cl concentrations was absolutely inhibited on Day 4. The photosynthesis rate as well as the maximum quantum efficiency of PSII also decreased by NH_4Cl. The Fv/Fm ratio is a fluorescence parameter that emits from microalgal cell emission. Generally, F_m (maximum fluorescence) level is generated by a short pulse (10,000 µmol photon s^{-1} m^{-2}). This pulse makes a high photon flux that drives the PSII reaction center into a closed state. F_0 (minimum fluorescence level) is generated by very low light intensity (dark). This situation makes all PSII reaction centers into an open state. The difference between F_0 and F_m is called Fv. The results showed that Fv/Fm ratio was significantly decreased under both 17 and 60 mM NH_4Cl conditions. Supporting the decrease in the maximum quantum efficiency of PSII, this study's proteomics analysis found that most of the identified photosynthetic proteins in PSII were downregulated in NH_4Cl supplementation (Fig. 6) because PSII proteins play an important role in nonphotochemical quenching [24].

Preprints (www.preprints.org) | NOT PEER-REVIEWED | Posted: 15 November 2022 doi:10.20944/preprints202211.0284.v1

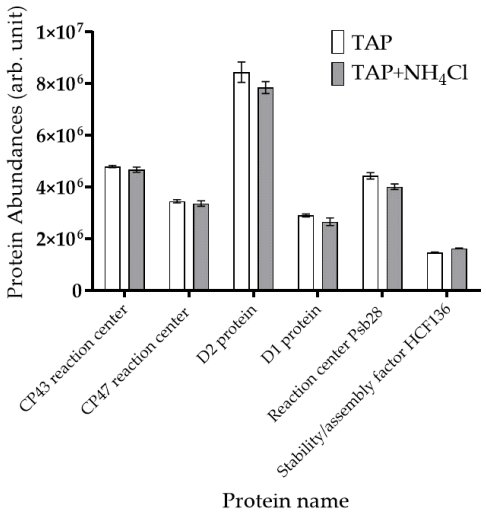

Figure 6. NH_4Cl's effect on PSII protein abundance. The bar graph represents the mean and CV of the LC-MS measurement (n = 3).

Decreasing these proteins groups can reduce plant photosynthesis. A combination of maximum quantum efficiency of PSII and proteomics results suggested an NH_4Cl decreased in photosynthesis efficiency. Further investigation of photosynthesis parameters showed that the ammonium supplementation under both conditions did not affect chlorophyll a and b content.

Based on this study's investigations, it can be suggested that NH_4Cl could affect photosynthesis activities by decreasing oxygen evolution and the maximum quantum efficiency of PSII and their protein abundance, but did not alter the photosynthesis pigments including chlorophyll a and b. Several studies have shown that that ionized ammonia ions can ligate to the photosystem II oxygen evolution reaction core, thereby creating increased photosensitivity that results in increased photosystem damage [11]. In *Arthrospira platensis*, ammonium ions could affect the oxygen evolution complex (OEC) in photosystems by displacing a water ligand at the OEC binding sites [10]. In addition, ammonium ions possibly inhibited ATP synthesis and induced extra NADPH production by uncoupling photophosphorylation and reduced the transthylakoid proton gradient [25]. Moreover, intracellular oxidative stress triggered by ammonium ions could impact the specific activities of antioxidant enzymes and even cause lipid peroxidation [26].

The proteomics analysis found unique and differentially expressed proteins in NH_4Cl conditions. Nuclear/nucleolar GTPase 2 is a unique marker protein in the NH_4Cl group. This protein is classified in the GTPases protein families [27]. They are essential for the biogenesis and assembly of ribosomal subunits in the eukaryote cells. In addition, they are involved in the regulatory processes in plant development [28]. For the significantly differentially expressed proteins, 2 important and well-characterized proteins were discovered including the putative acetate uptake transporter GFY5 and acyl-coenzyme A oxidase. The putative acetate uptake transporter GFY5 upregulation suggested that NH_4Cl supplementation could enhance the acetate ion uptake into the cells. Additionally, the acetate ion is a direct substrate of the lipid biosynthesis precursor. Fan and their collage showed that excess acetate supply resulted in significant TAG accumulation rather than the other conditions [21]. Another upregulated protein is acyl-coenzyme A oxidase. This protein is an enzyme that catalyzes the chemical reaction of acyl-CoA to *trans*-2, 3-dehydroacyl-CoA. This reaction occurs in peroxisomes and plays an essential role in the lipid metabolism of cells. This enzyme's function involves β-oxidation machinery in microalga for fatty acid breakdown in the mitochondria and peroxisomes [29]. On the one hand, inhibiting β-oxidation reaction can prevent lipid loss and result in intracellular acyl-CoA buildup, as observed in *Arabiopsis thaliana* mutants lacking ACOX [30]. Therefore, an

increase in β-oxidation reaction could provide for enhanced carbon skeleton recycling from degraded membrane lipids for TAG biosynthesis.

5. Conclusions

NH_4Cl supplementation effects on triglyceride induction in *C. reinhardtii* was successfully studied. Here NH_4Cl only induced triglycerides under mixotrophic cultivation but not under photoautotrophic conditions. Under mixotrophic cultivation, NH_4Cl has the potential to supplement for increasing biomass and lipid production in microalgal cultures. NH_4Cl was found to stimulate acetate transporter protein GFY5 expression. In addition, the global protein expression showed NH_4Cl affected the nitrogen metabolism pathway. This can lead us to more biochemical information for producing biofuel from microalga.

Author Contributions: Conceptualization, K.Y., Y.Y. and S.K.; Data curation, W.S.; Formal analysis, W.S.; Funding acquisition, W.S., K.Y., Y.Y. and S.K.; Investigation, W.S.; Methodology, W.S. and C.A.; Project administration, Y.Y. and S.K.; Resources, K.Y., Y.Y. and S.K.; Software, C.A.; Supervision, C.A., Y.Y. and S.K.; Validation, W.S. and C.A.; Writing – original draft, W.S.; Writing – review & editing, W.S. and S.K.

Funding: This research is financially supported by the 2020 Graduate Development Scholarship (No), offered by the National Research Council of Thailand.

Acknowledgments: This research is financially supported by the 2020 Graduate Development Scholarship (No), offered by the National Research Council of Thailand.

Conflicts of Interest: The authors declare no conflict of interest. The funder had no role in the experimental designs, in the data collection, interpretation of data, in the writing of the manuscript, and in the decision to publish the results.

References

1. Lobo-Moreira, A.B.; Xavier-Santos, S.; Damacena-Silva, L.; Caramori, S.S. Trends on Microalgae-Fungi Consortia Research: An Alternative for Biofuel Production? *Front Microbiol* **2022**, *13*, 903737, doi:10.3389/fmicb.2022.903737.
2. Ganesan, R.; Manigandan, S.; Samuel, M.S.; Shanmuganathan, R.; Brindhadevi, K.; Lan Chi, N.T.; Duc, P.A.; Pugazhendhi, A. A review on prospective production of biofuel from microalgae. *Biotechnol Rep (Amst)* **2020**, *27*, e00509, doi:10.1016/j.btre.2020.e00509.
3. Alishah Aratboni, H.; Rafiei, N.; Garcia-Granados, R.; Alemzadeh, A.; Morones-Ramirez, J.R. Biomass and lipid induction strategies in microalgae for biofuel production and other applications. *Microb Cell Fact* **2019**, *18*, 178, doi:10.1186/s12934-019-1228-4.
4. El-Sheekh, M.M.; Gheda, S.F.; El-Sayed, A.E.B.; Abo Shady, A.M.; El-Sheikh, M.E.; Schagerl, M. Outdoor cultivation of the green microalga Chlorella vulgaris under stress conditions as a feedstock for biofuel. *Environ Sci Pollut Res Int* **2019**, *26*, 18520-18532, doi:10.1007/s11356-019-05108-y.
5. Ahmed, R.A.; He, M.; Aftab, R.A.; Zheng, S.; Nagi, M.; Bakri, R.; Wang, C. Bioenergy application of Dunaliella salina SA 134 grown at various salinity levels for lipid production. *Sci Rep* **2017**, *7*, 8118, doi:10.1038/s41598-017-07540-x.
6. Hu, Q.; Sommerfeld, M.; Jarvis, E.; Ghirardi, M.; Posewitz, M.; Seibert, M.; Darzins, A. Microalgal triacylglycerols as feedstocks for biofuel production: perspectives and advances. *The Plant Journal* **2008**, *54*, 621-639, doi:https://doi.org/10.1111/j.1365-313X.2008.03492.x.
7. Bibi, F.; Jamal, A.; Huang, Z.; Urynowicz, M.; Ishtiaq Ali, M. Advancement and role of abiotic stresses in microalgae biorefinery with a focus on lipid production. *Fuel* **2022**, *316*, 123192, doi:https://doi.org/10.1016/j.fuel.2022.123192.
8. You, J.; Chan, Z. ROS Regulation During Abiotic Stress Responses in Crop Plants. *Front Plant Sci* **2015**, *6*, 1092, doi:10.3389/fpls.2015.01092.
9. Yaakob, M.A.; Mohamed, R.M.S.R.; Al-Gheethi, A.; Aswathnarayana Gokare, R.; Ambati, R.R. Influence of Nitrogen and Phosphorus on Microalgal Growth, Biomass, Lipid, and Fatty Acid Production: An Overview. *Cells* **2021**, *10*, 393, doi:10.3390/cells10020393.
10. Markou, G.; Vandamme, D.; Muylaert, K. Ammonia inhibition on Arthrospira platensis in relation to the initial biomass density and pH. *Bioresour Technol* **2014**, *166*, 259-265, doi:10.1016/j.biortech.2014.05.040.
11. Drath, M.; Kloft, N.; Batschauer, A.; Marin, K.; Novak, J.; Forchhammer, K. Ammonia triggers photodamage of photosystem II in the cyanobacterium Synechocystis sp. strain PCC 6803. *Plant Physiol* **2008**, *147*, 206-215, doi:10.1104/pp.108.117218.
12. Li, J.; Wang, L.; Lu, Q.; Zhou, W. Toxicity alleviation for microalgae cultivation by cationic starch addition and ammonia stripping and study on the cost assessment. *RSC Adv* **2019**, *9*, 38235-38245, doi:10.1039/c9ra03454d.

13. Li, X.; Li, W.; Zhai, J.; Wei, H.; Wang, Q. Effect of ammonium nitrogen on microalgal growth, biochemical composition and photosynthetic performance in mixotrophic cultivation. *Bioresour Technol* **2019**, *273*, 368-376, doi:10.1016/j.biortech.2018.11.042.
14. Li, X.; Lu, Y.; Li, N.; Wang, Y.; Yu, R.; Zhu, G.; Zeng, R.J. Mixotrophic Cultivation of Microalgae Using Biogas as the Substrate. *Environ Sci Technol* **2022**, *56*, 3669-3677, doi:10.1021/acs.est.1c06831.
15. Lichtenthaler, H.K.; Buschmann, C. Chlorophylls and Carotenoids: Measurement and Characterization by UV-VIS Spectroscopy. *Current Protocols in Food Analytical Chemistry* **2001**, *1*, F4.3.1-F4.3.8, doi:https://doi.org/10.1002/0471142913.faf0403s01.
16. Krobthong, S.; Yingchutrakul, Y.; Samutrtai, P.; Hitakarun, A.; Siripattanapipong, S.; Leelayoova, S.; Mungthin, M.; Choowongkomon, K. Utilizing Quantitative Proteomics to Identify Species-Specific Protein Therapeutic Targets for the Treatment of Leishmaniasis. *ACS Omega* **2022**, doi:10.1021/acsomega.1c05792.
17. Krobthong, S.; Yingchutrakul, Y.; Visessanguan, W.; Mahatnirunkul, T.; Samutrtai, P.; Chaichana, C.; Papan, P.; Choowongkomon, K. Study of the Lipolysis Effect of Nanoliposome-Encapsulated Ganoderma lucidum Protein Hydrolysates on Adipocyte Cells Using Proteomics Approach. *Foods* **2021**, *10*, 2157.
18. Shilov, I.V.; Seymour, S.L.; Patel, A.A.; Loboda, A.; Tang, W.H.; Keating, S.P.; Hunter, C.L.; Nuwaysir, L.M.; Schaeffer, D.A. The Paragon Algorithm, a Next Generation Search Engine That Uses Sequence Temperature Values and Feature Probabilities to Identify Peptides from Tandem Mass Spectra*. *Molecular & Cellular Proteomics* **2007**, *6*, 1638-1655, doi:https://doi.org/10.1074/mcp.T600050-MCP200.
19. Willforss, J.; Chawade, A.; Levander, F. NormalyzerDE: Online Tool for Improved Normalization of Omics Expression Data and High-Sensitivity Differential Expression Analysis. *J Proteome Res* **2019**, *18*, 732-740, doi:10.1021/acs.jproteome.8b00523.
20. Lee, S.-A.; Ko, S.-R.; Lee, N.; Lee, J.-W.; Le, V.V.; Oh, H.-M.; Ahn, C.-Y. Two-step microalgal (Coelastrella sp.) treatment of raw piggery wastewater resulting in higher lipid and triacylglycerol levels for possible production of higher-quality biodiesel. *Bioresource Technology* **2021**, *332*, 125081, doi:https://doi.org/10.1016/j.biortech.2021.125081.
21. Fan, J.; Yan, C.; Andre, C.; Shanklin, J.; Schwender, J.; Xu, C. Oil accumulation is controlled by carbon precursor supply for fatty acid synthesis in Chlamydomonas reinhardtii. *Plant and Cell Physiology* **2012**, *53*, 1380-1390, doi:10.1093/pcp/pcs082.
22. Goodson, C.; Roth, R.; Wang, Z.T.; Goodenough, U. Structural correlates of cytoplasmic and chloroplast lipid body synthesis in Chlamydomonas reinhardtii and stimulation of lipid body production with acetate boost. *Eukaryot Cell* **2011**, *10*, 1592-1606, doi:10.1128/EC.05242-11.
23. Lin, W.; Li, P.; Liao, Z.; Luo, J. Detoxification of ammonium to Nannochloropsis oculata and enhancement of lipid production by mixotrophic growth with acetate. *Bioresour Technol* **2017**, *227*, 404-407, doi:10.1016/j.biortech.2016.12.093.
24. Cazzaniga, S.; Kim, M.; Bellamoli, F.; Jeong, J.; Lee, S.; Perozeni, F.; Pompa, A.; Jin, E.; Ballottari, M. Photosystem II antenna complexes CP26 and CP29 are essential for nonphotochemical quenching in Chlamydomonas reinhardtii. *Plant Cell Environ* **2020**, *43*, 496-509, doi:10.1111/pce.13680.
25. Collos, Y.; Harrison, P.J. Acclimation and toxicity of high ammonium concentrations to unicellular algae. *Mar Pollut Bull* **2014**, *80*, 8-23, doi:10.1016/j.marpolbul.2014.01.006.
26. Nimptsch, J.; Pflugmacher, S. Ammonia triggers the promotion of oxidative stress in the aquatic macrophyte Myriophyllum mattogrossense. *Chemosphere* **2007**, *66*, 708-714, doi:10.1016/j.chemosphere.2006.07.064.
27. Woollard, A.A.; Moore, I. The functions of Rab GTPases in plant membrane traffic. *Curr Opin Plant Biol* **2008**, *11*, 610-619, doi:10.1016/j.pbi.2008.09.010.
28. Du, C.; Chong, K. ARF-GTPase activating protein mediates auxin influx carrier AUX1 early endosome trafficking to regulate auxin dependent plant development. *Plant Signal Behav* **2011**, *6*, 1644-1646, doi:10.4161/psb.6.11.17755.
29. Kong, F.; Liang, Y.; Légeret, B.; Beyly-Adriano, A.; Blangy, S.; Haslam, R.P.; Napier, J.A.; Beisson, F.; Peltier, G.; Li-Beisson, Y. Chlamydomonas carries out fatty acid β-oxidation in ancestral peroxisomes using a bona fide acyl-CoA oxidase. *The Plant Journal* **2017**, *90*, 358-371, doi:https://doi.org/10.1111/tpj.13498.
30. Rylott, E.L.; Rogers, C.A.; Gilday, A.D.; Edgell, T.; Larson, T.R.; Graham, I.A. Arabidopsis mutants in short- and medium-chain acyl-CoA oxidase activities accumulate acyl-CoAs and reveal that fatty acid beta-oxidation is essential for embryo development. *J Biol Chem* **2003**, *278*, 21370-21377, doi:10.1074/jbc.M300826200.